

Provided for non-commercial research and educational use only.  
Not for reproduction or distribution or commercial use.



This article was originally published in a journal published by Elsevier, and the attached copy is provided by Elsevier for the author's benefit and for the benefit of the author's institution, for non-commercial research and educational use including without limitation use in instruction at your institution, sending it to specific colleagues that you know, and providing a copy to your institution's administrator.

All other uses, reproduction and distribution, including without limitation commercial reprints, selling or licensing copies or access, or posting on open internet sites, your personal or institution's website or repository, are prohibited. For exceptions, permission may be sought for such use through Elsevier's permissions site at:

<http://www.elsevier.com/locate/permissionusematerial>



# A surface-tethered model to assess size-specific effects of hyaluronan (HA) on endothelial cells

Samir Ibrahim<sup>a</sup>, Binata Joddar<sup>a</sup>, Matthew Craps<sup>b</sup>, Anand Ramamurthi<sup>a,c,\*</sup>

<sup>a</sup>Department of Bioengineering, Clemson University, 501 Rhodes Research Center, Clemson, SC 29634, USA

<sup>b</sup>Department of Physics and Astronomy, Clemson University, 118 Kinard Laboratory, Clemson, SC 29634, USA

<sup>c</sup>Department of Cell Biology and Anatomy, Medical University of South Carolina, 173 Ashley Avenue, Basic Science Building 601, Charleston, SC 29425, USA

Received 15 June 2006; accepted 20 September 2006

Available online 11 October 2006

## Abstract

Crosslinked gels (hyalans) containing long-chain ( $MW > 1 \times 10^6$  Da) hyaluronan (HA), a connective tissue GAG, show exceptional biocompatibility for vascular implantation but poorly interact with vascular endothelial cells (ECs). Previous studies showed in situ fragmentation of HA by UV light to bioactivate hylan gels and elicit enhanced EC responses. Since fragmented HA can be pro-inflammatory, it is important to define an optimal size distribution of HA fragments on the hylan surface that will recruit and support normally functional ECs and limit ulterior responses. Related studies have shown that exogenous models of HA do not necessarily replicate cell responses to HA scaffolds. Since scaffolds cannot be created based on fragmented HA alone, we sought to determine size-specific responses of ECs to HA substrates of defined fragment sizes by creation of HA-tethered culture surfaces. HA (1000, 200, 20 kDa) and an oligomer mixture were tethered onto an aminosilane (APTMS)-treated glass surfaces using a carbodiimide reaction. MALDI-TOF showed the HA digests to contain HA 4–8mers with a  $75 \pm 0.4\%$  w/w of 4mers. Immuno-fluorescence, SEM, AFM and XPS analysis revealed homogeneous amine and HA surfaces. An amine s-SDTB assay and HA fluorophore-assisted carbohydrate electrophoresis (FACE) indicated surface densities of  $9 \pm 3$  amine groups/nm<sup>2</sup> and  $0.57 \pm 0.44$   $\mu\text{g}/\text{cm}^2$ , respectively. HA/HA fragments/oligomers were stable over 21 days of incubation in serum-free culture media. EC proliferation on these surfaces resulted was limited, a possible effect of smooth surface topography, high anionicity, and in case of 4mers, non-interaction with primary HA cell-surface receptors (CD44). This work is significant in that it allows testing of cell responses to substrates composed of single-sized fragments of HA that cannot by themselves be cross-linked into a gel. Future work in our lab will use this model to assess the effects of other HA oligomer sizes on EC behavior.

© 2006 Elsevier Ltd. All rights reserved.

**Keywords:** Hyaluronic acid; Oligomers; FACE; SEM; AFM; XPS

## 1. Introduction

The extracellular matrix (ECM), once regarded simply as a structural scaffold, is now recognized as an important modulator of cell phenotype and function. From the tissue engineering perspective, it is increasingly apparent that ECM molecules provide the necessary biomechanical and biochemical stimulation of cultured cells to create an

environment similar to native tissues. A class of ECM molecules that are increasingly studied in the context of cell culture scaffolds are glycosaminoglycans (GAGs). One such GAG, hyaluronic acid (HA), occurs naturally in connective tissues (e.g., skin) as a simple linear molecule consisting of repeating disaccharide units of *N*-acetyl-D-glucosamine and D-glucuronic acid [1]. Most cells have the ability to synthesize HA at some point during their cell cycle, implicating its function in several fundamental biological processes [2].

In recent years, hyaluronan has been recognized as a biomaterial for potentially effective tissue regeneration. It is now known that HA, when degraded into small fragment

\*Corresponding author. Department of Bioengineering, Clemson University, 501 Rhodes Research Center, Clemson, SC 29634, USA. Tel.: +1 843 792 5853; fax: +1 843 792 0664.

E-mail address: [aramamu@clemson.edu](mailto:aramamu@clemson.edu) (A. Ramamurthi).

sizes, plays a role in wound healing by promoting angiogenesis [3]. HA fragments can, under specific circumstances, also promote early inflammation, which is critical to initiate wound healing, which can then modulate later stages of the process, allowing for matrix stabilization and reduction of long-term inflammation [2]. HA is also highly biocompatible and does not elicit a foreign-body response upon cross-transplantation due to the homology of the HA structure across species [2]. Although the mechanism of interaction between HA and the human body is still incompletely elucidated, its promising characteristics have assured its extensive use as a tissue engineering scaffold, most recently for cartilage [4] and skin repair [5].

Our lab is currently investigating the potential use of HA as small diameter vascular graft materials. It is generally understood that complete endothelialization of the graft lumen is essential to ensure long-term patency of vascular grafts and thus key to the long-term success of intravascular implants. HA has been shown to exhibit a size-specificity in modulating endothelial cell (EC) proliferation, key to successful graft endothelialization. Exogenous HA oligomers have been shown to stimulate angiogenesis [6] and proliferation of vascular ECs [7], while high molecular weight (HMW) HA ( $MW > 1 \times 10^6$  Da) generally have the opposite effect [8]. In a prior study, we also demonstrated similar cell responses atop HA-based hydrogels [9].

Our previous studies with divinyl sulfone (DVS)-cross-linked HA hydrogels (hylans), composed of HMW HA alone, showed them to be bioinert and non-conductive to cell spreading and proliferation. However, such gels could be bio-activated by controlled irradiation with UV light, a process that splices HMW HA to create a ranged of sized HA fragments, including HA oligomers [9]. It was observed that vascular ECs readily attach, spread, proliferate and generally exhibit a healthy phenotype and functionality when cultured atop these bio-activated gels. Since the effects of UV light can be difficult to control, and can potentially cause random ionizations that are structurally disruptive, a better approach is to create 'bioactivated' gels containing bio-inert long-chain HA, necessary to maintain mechanical integrity and biocompatibility, and smaller, more cell-interactive HA fragments/oligomers. In pursuing this approach, it is, however, important to incorporate optimally sized HA fragments, and modulate their content within the HA biomaterial such as to evoke desired cell responses, and yet prevent exaggerated responses (e.g., inflammation, hyper-proliferation) that can be potentially elicited by HA fragments. From the perspective of developing HA biomaterials for vascular applications, we thus seek to methodically elucidate the impact of HA, its large fragments, and oligomers on vascular EC phenotype, functionality and gene expression.

It was clear from our previous studies [9,10] that while exogenous supplementation models broadly predict cell responses to substrate/scaffold components, presentation

of these very components to cells, immobilized on a 2-D substrate, may more closely simulate cell responses within 3-D scaffolds due to the intimate cell contact with substrate-bound HA (rather than periodic contact with HA medium supplements). This study thus describes our attempts to immobilize HA, in a wide range of fragment sizes, on 2-D glass surfaces and test EC responses to these molecules.

## 2. Materials and methods

### 2.1. Preparation of HA oligomer mixtures

HA 1000 was enzymatically digested to produce a mixture of HA oligomers. Briefly, HA 1000 was digested (37 °C, 18 h) with bovine *Testicular hyaluronidase*, (Sigma, 40 U/mg) in a 5 mg/ml solution of digest buffer (150 mM NaCl, 100 mM CH<sub>3</sub>COONa, 1 mM Na<sub>2</sub>-EDTA, pH 5.0) at 37 °C for 18 h. The enzyme was then precipitated, its activity terminated by boiling (2 min), and cooled on ice. Following centrifugation (2800 rpm, 10 min), to separate the enzyme from the mixture, the supernatant was dialyzed in water (12 h) using dialysis cassettes (Pierce Biotechnology Inc.) with a MW cut-off of 2 kDa, and then freeze-dried overnight to generate lyophilized HA oligomers.

### 2.2. MALDI-TOF MS analysis

MALDI-TOF MS analyses of HA oligomers were performed on a Voyager-DE STR Biospectrometry Workstation (Applied Biosystems, Foster City, CA) in a linear mode. The MALDI matrix used for sample analysis was  $\alpha$ -cyano-4-hydroxycinnamic acid (8 mg/ml in 50% v/v acetonitrile, 0.3% v/v trifluoroacetic acid). Samples (2  $\mu$ l) containing equal volumes of matrix and sample solution were coated and air-dried onto a stainless steel target. Positive spectra were recorded in a linear mode using the minimum laser energy required to give an observable signal ( $\sim 10:1$  signal: noise). All sample digests ( $n = 3$ /condition) were each analyzed in at least triplicate using MALDI-TOF. The commercial HA oligomer preparations were also similarly analyzed for fragment size distribution ( $n = 3$ /condition).

### 2.3. Immobilization of HA, HA fragments and oligosaccharides

HMW HA, large HA fragments, and HA oligomers were tethered onto glass surfaces using a carbodiimide linking chemistry [11]. HA 1000 (1000 kDa; Fluka, Milwaukee, WI), HA 200 (200 kDa; Genzyme, Cambridge, MA), HA 20 (20 kDa; Lifecore Biomedical, Chaska, MN), and in-house prepared oligomer mixtures (see Section 2.1) were immobilized onto 4-well glass chamber slides (Nalge Nunc International, Naperville, IL). The chamber slides were incubated in 1 M NaOH for 1 h to de-protonate the exposed hydroxyl groups and render the glass surface uniformly reactive. The glass surface was rinsed with DI water and 95% v/v ethanol (Sigma, St Louis, MO), and then activated by incorporation of aminosilanes. A 3% v/v solution of 3-aminopropyl-trimethoxysilane (APTMS; Fluka Chemical Corp., Milwaukee, WI) in 95% v/v ethanol was prepared and the silane was allowed to convert into silanol over 5 min. A 1-ml aliquot of the solution was then reacted with the glass slide (30 min, 23 °C) with shaking. The slides were then briefly rinsed in 100% v/v ethanol (Sigma), dried under a steady stream of argon gas, and finally heated in an oven (1 h, 115 °C), rinsed three times with 95% v/v ethanol, and dried again under argon gas.

Immobilized amines were covalently reacted with the carboxyl groups present on HA, using a carbodiimide reaction. Briefly, an aqueous HA solution (3 mg/ml) was prepared with 200 mM 1-Ethyl-3-[3-dimethylaminopropyl]carbodiimide (EDC) hydrochloride (Pierce Biotechnology Inc., Rockford, IL) and 100 mM *N*-hydroxysuccinimide (NHS; Pierce Biotechnology Inc.). A 1-ml aliquot of this solution was applied to each well and

allowed to react for 16 h with continuous agitation on a shaker. The slides were then soaked in DI water for 2 h to remove unbound HA, and finally air-dried under argon gas.

#### 2.4. Sulfo-succinimidyl-4-O-(4,4'-dimethoxytrityl)-butyrate assay for quantification of tethered amine groups

Aminosilane surfaces were washed with 50 mM sodium  $\text{NaHCO}_3$  buffer, pH 8.5. A 1-ml aliquot of this buffer containing 2% v/v dimethyl formamide (DMF) and 0.1 mM sulfo-succinimidyl-4-O-(4,4'-dimethoxytrityl)-butyrate (s-SDTB) was incubated (30 min, 23 °C) with each well of the aminosilanated chamber slides to allow s-SDTB to bind to the exposed amine groups. The slides were then gently rinsed with methanol to remove unreacted s-SDTB, and then treated with a 50% v/v solution of 60% v/v perchloric acid in methanol (10 min, 23 °C) to elute the 4, 4'-dimethoxytrityl cation from the bound s-SDTB. The amount of cation was measured using a spectrophotometer (Molecular Devices, Sunnyvale, CA) at  $\lambda = 498$  nm. The concentration of the cation, and hence surface amines, was determined by comparison of the unknowns with a calibration curve generated with known amounts of 4, 4'-dimethoxytrityl chloride prepared in perchloric acid/methanol solution.

#### 2.5. Fluorescence microscopy

Successful surface-immobilization of amines was confirmed by fluorescence labeling with a Alexa-488-conjugated amine-reactive dye (Molecular Probes, Temecula, CA; 1:1000 v/v in  $\text{NaHCO}_3$  buffer, pH 8.5). Surface-bound HA/HA fragments were detected by immunofluorescence, either using a biotinylated HA binding protein (HABP) and rhodamine-conjugated streptavidin, or with FITC-pre-conjugated HA. A solution of biotinylated-HABP (b-HABP; 0.5 mg/ml, diluted 1:100 in PBS; Associates of Cape Cod, E. Falmouth, MA) was added to the slide chambers and allowed to react with the HA-tethered surfaces (1 h). Excess b-HABP was removed by rinsing with PBS. A solution of bovine serum albumin (BSA; 5% v/v in PBS) was added to the slides as a blocking agent (20 min). The slides were then again washed with PBS to remove the blocker. Texas Red-conjugated neutravidin (Molecular Probes; 1:500 v/v in PBS) was allowed to react with the b-HABP on HA (1 h, dark). The solution was then aspirated, the surfaces washed with PBS and DI water, and the slides mounted with Vectashield. The negative control was not treated with HABP. The slides were imaged using a confocal microscope (Leica TCS SP2 AOBS, Allendale, NJ).

#### 2.6. Scanning electron microscopy

Glass, aminosilanated glass, and HA-tethered glass surfaces were visualized using scanning electron microscopy (SEM) to assess the homogeneity of the coated layers. Argon-dried surfaces were coated with gold (60 s) in a sputter coater (VG-Microtech, Uckfield, UK) and visualized using a SEM 3500 (Hitachi Ltd, Tokyo, Japan) at  $150 \times$  to  $1500 \times$  magnification.

#### 2.7. Atomic force microscopy

Atomic force microscopy (AFM) was performed on glass, aminosilane and HA-tethered substrates to determine the surface roughness and gauge the uniformity of the coatings at the cellular (micron) scale. Argon-dried surfaces were analyzed using a Digital Instruments CP-II (Veeco, Woodbury, NY) AFM equipped with an Ultralever contact mode tip (Veeco, Woodbury, NY) and titanium cantilever. Three areas per sample were imaged under contact mode and analyzed with Proscan 1.9 and Image Analysis 2.1 to obtain a line scan section profile used to measure the peak heights.

#### 2.8. X-ray photoelectron spectroscopy

X-ray photoelectron spectroscopy (XPS) was used to compare the elemental composition and chemical structure characteristics of the glass, aminosilane and HA-coated surfaces. Dried slides were stored in a desiccator prior to analysis using an Axis 165 XPS system (Kratos, Chestnut Ridge, NY) with a monochromatic aluminum target X-ray source (15 kV and 10 mA). Samples were analyzed at a pressure of  $10^{-9}$  Torr and temperature of 23 °C with a takeoff angle close to 0°. Scans between 1200 and 0 eV were performed and the resulting spectra were referenced to the substrate C 1 s peak. Higher resolution spectra were also generated to monitor the formation of functional groups upon HA immobilization.

#### 2.9. Assays for quantification of HA loss from the surface

Loss of surface-bound HA was assessed over 3 weeks of incubation in serum-free culture medium by a colorimetric toluidine blue assay and Fluorophore-Assisted Carbohydrate Electrophoresis (FACE). For both tests, HA-coated surfaces were incubated in culture media (MCDB-131, Invitrogen, Carlsbad, CA; 37 °C) for 0, 1, 4, 7, 14, and 21 days. On the respective days, the medium was aspirated and a 500  $\mu\text{l}$  aliquot of an aqueous solution of toluidine blue (0.075 mg/ml) was added to the HA surfaces and agitated on a shaker for 10 min. The absorbance of the solution, following removal toluidine blue by binding to surface-tethered HA, was measured spectrophotometrically at  $\lambda = 630$  nm.

FACE analysis was used to quantify the amount of HA/HA fragments remaining on the slide surface after 1, 14 and 21 days of incubation with culture medium. In preparation for FACE, 20 mU of *hyaluronidase SD* (Associates of Cape Cod, East Falmouth, MA) solubilized in 0.1 M ammonium acetate, pH 7.0, was added to each well of the chamber slide and incubated (37 °C, 6 h) to digest HA off the surfaces. The resulting solution, containing HA disaccharides ( $\Delta\text{DiHA}$ ), was freeze-dried and then re-suspended in 40  $\mu\text{l}$  of 0.0125 M solution of the fluorescent dye 2-aminoacridone (AMAC, Sigma) prepared in acetic acid/DMSO (3:17 v/v) and incubated (23 °C, 15 min, dark). A 40  $\mu\text{l}$  aliquot of an aqueous solution of 1.25 M sodium cyanoborohydride (Sigma) was then added to each sample and incubated (37 °C, 16 h, dark). Following this, 20  $\mu\text{l}$  of glycerol was added to each sample. Standards were also prepared using known amounts of commercially available HA disaccharides (V-Labs, Covington, LA). If necessary, samples were stored at  $-20$  °C, prior to use.

For electrophoresis, all 8 lanes of a polyacrylamide MONO<sup>®</sup> gel (Glyko, San Leandro, CA) were loaded simultaneously with 4  $\mu\text{l}$  of sample/standard using an 8-channel glass syringe (Hamilton, Reno, NV) and run with MONO<sup>®</sup> gel running buffer (Glyko), as adopted from a previously published method [12]. Briefly, the electrophoresis apparatus (Glyko) was placed in a trough of ice to maintain the buffer temperature below 10 °C throughout the electrophoresis process. Samples were electrophoresed at a constant 500 V with a starting current of 25 mA/gel and a final current of 10 mA/gel for 80 min. After electrophoresis, the gels were illuminated with UV-B light ( $\lambda = 365$  nm) in a FluorChem 8900 (Alpha Innotech, San Leandro, CA) and the band intensities were quantified and compared to the standard to calculate the amount of  $\Delta\text{DiHA}$  present.

#### 2.10. Cell culture and analysis

Preliminary studies with rat aortic ECs were performed to assess the retention and proliferation of cells cultured on the HA surfaces. Adult rat aortic ECs (RAEC, passage 6–8; Cell Applications, San Diego, CA) were trypsinized (0.25% trypsin/0.1% v/v EDTA; Invitrogen), pelleted by centrifugation (500g, 7 min), re-suspended in MCDB-131 supplemented with 10% v/v FBS (Invitrogen), 1% v/v penicillin-streptomycin (Invitrogen), 50  $\mu\text{g}/\text{ml}$  EC growth supplement (Becton Dickinson, Franklin Lakes, NJ), 4 mmol/L L-glutamine (Invitrogen), and 30 U/ml heparin (Sigma) and seeded onto glass, aminosilane and HA-coated chamber slide surfaces. Fibronectin coated 4-well chamber slides were used as a positive control.

Spent medium was replaced twice weekly during the duration of culture, up to 21 days. The DNA content of the EC monolayers was used to assess the proliferation of ECs in culture at 1, 4, 14 and 21 days using the fluorometric method described by Labarca and Paigen [13]. Cell numbers were calculated from measured DNA content assuming 6 pg DNA/cell [13].

### 2.11. Statistical analysis

All experiments were performed in triplicate, unless otherwise mentioned. Statistical significance between and within groups was determined using Microsoft Excel's statistical function for *t*-tests, assuming unequal variance and two-tailed distribution. Differences were considered statistically significant at  $p < 0.05$ . Quantitative results are reported as mean  $\pm$  standard deviation.

## 3. Results

### 3.1. Characterization of HA oligomers

MALDI-TOF spectra of replicate aliquots of HA digests (40 U of enzyme/mg HA, 18 h, 37 °C) consistently yielded a narrow range of HA oligomers (4–8mers,  $MH^+ = 657$ –2172 Da; Fig. 1). The predominant peak % intensity corresponded to HA oligomers of size  $MH^+ = 657$  Da, i.e., the 4mer. Tested control aliquots (digest buffer with no HA) yielded several peaks (170–192 Da), all of much lower intensity and of smaller sizes than the desired peaks in the oligomer size range.

MALDI-TOF was also used to compare the % peak intensity of HA 4mer peaks generated in digests of both commercial preparations and in-house prepared oligomer

mixtures (2  $\mu$ g HA/ml). The intensity of the lone peak corresponding to the 4mer in the commercial preparation was considered 100% w/v pure for purpose of comparison. In comparison, the % peak intensity for the 4mer component of the in-house prepared oligomer mixture was  $75 \pm 0.4\%$  w/w.

### 3.2. Surface characterization

#### 3.2.1. Characterization of the aminosilane surface

An amine reactive dye was initially used to determine the presence of primary amines on the glass surface after treatment with the aminosilane. The silanated surface fluoresced brightly and uniformly indicating homogeneous tethering of amines (data not shown). SEM and AFM micrographs (Figs. 3B, 4B) and XPS spectra (Fig. 5, Table 1) confirmed the existence of a homogeneously distributed silane coating, distinctly different from glass surfaces (Figs. 3A, 4A). The s-SDTB amine assay indicated a surface amine density of  $9 \pm 3$  amine groups/nm<sup>2</sup>.

#### 3.2.2. Microscopic visualization of HA-coated surfaces

The presence of HA, or its fragments (HA 1000, HA 200, HA 20) chemically bound to the surface-tethered amine groups was confirmed by red fluorescence (Figs. 2A–C). HA 1000 surfaces appeared somewhat less homogeneous with some gaps between areas of intense fluorescence while the HA 200 and HA 20 surfaces fluoresced more uniformly. Controls, untreated with biotinylated HABP, did not fluoresce (Fig. 2E). Fluorescently tagged HA 90 immobilized onto the chamber slides also appeared coated on the glass substrates (Fig. 2D) similar to HA 20. Controls were FITC-treated aminosilanated glass (Fig. 2F).

Scanning electron micrographs of the glass surfaces showed random circular patches, a likely attribute of commercial plasma treatment (Fig. 3A). On silane-treated surfaces, these speckled patches were not seen although other structures, assumably aminosilane molecules, were seen across all replicate samples indicating a successful silane coating (Fig. 3B). HA-coated surfaces (Figs. 3C–F) were void of these structures, but instead showed smooth (HA 1000) or more fenestrated (HA 200, HA 20, HA 4mer) sheets, not seen on untreated glass and aminosilanated glass.

AFM also conclusively demonstrated the presence of tethered aminosilanes, HA and HA fragments and, for the most part, their formation of homogeneous layers. The increase in average peak height (roughness) of the aminosilane-treated surfaces ( $0.1305 \pm 0.0695 \mu$ m) in comparison to untreated glass ( $0.004 \pm 0.001 \mu$ m), as indicated by AFM, confirmed the successful immobilization of the aminosilane. The roughness of the HA surfaces showed an inverse correlation to molecular weight of HA fragments (Fig. 4). The average peak height atop surfaces coated with HA 1000, HA 200, HA 20 and HA 4mer were  $0.09142 \pm 0.06699$ ,  $0.4934 \pm 0.2002$ ,  $0.8345 \pm 0.3771$  and  $0.8871 \pm 0.3734 \mu$ m, respectively ( $n = 3$ /surface).

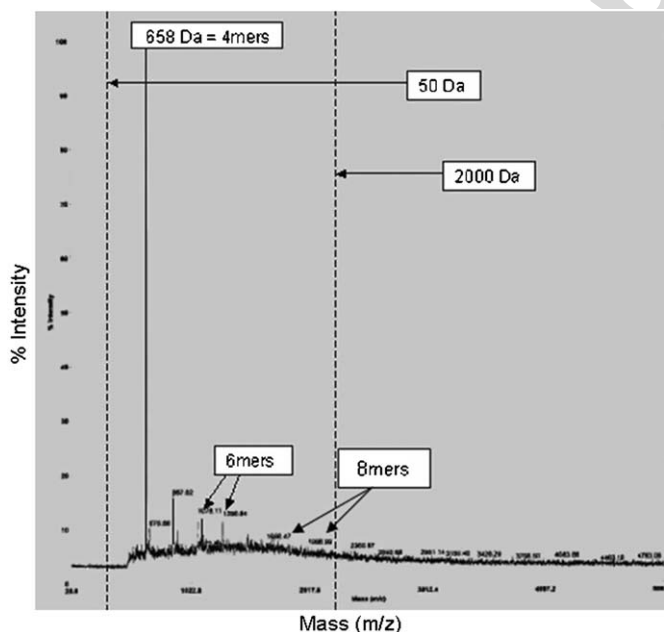


Fig. 1. MALDI-TOF spectra of *T. hyaluronidase* digests of long-chain HA. Digestion resulted in a mixture of HA oligomers in the range of 4–8mers. The major peak corresponds to the 4mer, while the smaller peaks indicate the presence of 6-mer and 8-mer HA. This by comparison with the spectrum of a pure 4-mer solution the 4-mer content in the mixture was estimated to be  $75 \pm 0.4\%$  w/w ( $n = 9$ ).

Table 1  
XPS analysis of glass, amine-bound and HA-bound surfaces and the corresponding theoretically predicted elemental profiles

	XPS atomic composition (%)			
	Si	O	C	N
<i>Surface</i>				
Glass	26.3±0.2	66.5±0.4	5.9±0.4	—
APTMS	11.0±0.2	23.8±1.4	53.0±1.0	12.1±0.4
HA 1000	1.5±1.7	29.7±2.5	57.6±1.7	11.2±2.1
HA 200	0.6±0.4	28.8±2.6	59.9±1.0	10.7±2.0
HA 20	2.0±0.7	24.4±0.8	68.6±1.8	5.0±1.9
HA 4mer	2.9±0.3	23.0±1.2	65.4±0.6	8.3±0.9
<i>Substance</i>				
Quartz	66.6	33.3	—	—
APTMS	9.1	27.3	54.5	9.1
HA	—	42.3	53.8	3.8

Glass is composed primarily of oxygen and silicon. An increase in carbon and decrease in silicon is observed with the introduction of APTMS, a carbon based structure. Likely, the large chains of HA 1000 and HA 200 significantly block the detection silicon while a substantial spectral peak corresponding elemental nitrogen was still observed. The smaller chains of HA 20 and HA 4mer allowed enhanced detection of elemental silicon but reduced the nitrogen peak. Results represent mean ±SD of readings obtained from  $n = 2$  regions/sample with a total of  $n = 4$  samples/substrate.

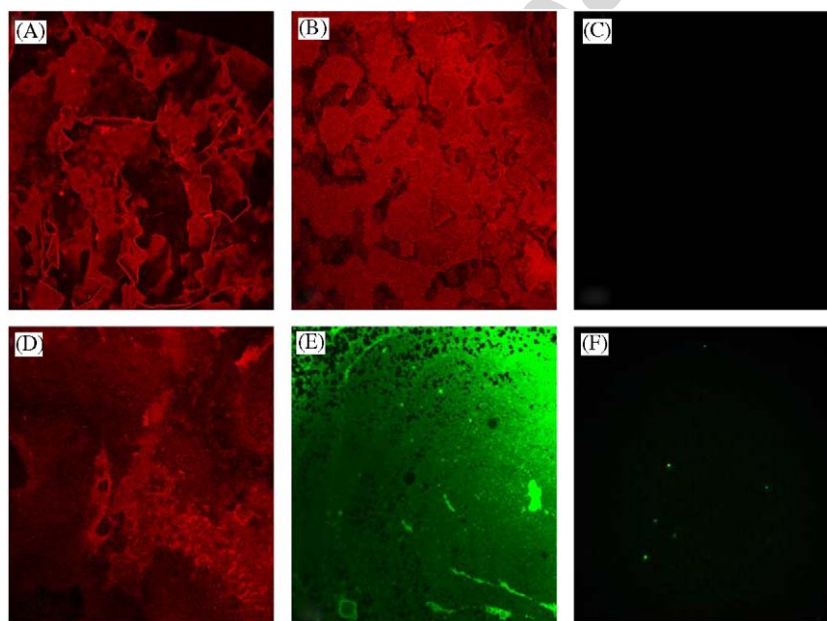


Fig. 2. Immunofluorescence detection of surface-immobilized HA. HA 1000, HA 200, and HA 20 were tagged with b-HABP and a rhodamine-conjugated streptavidin and appear homogeneously coated (red) on the surface (A–C). FITC-conjugated HA (MW 90 kDa) was also uniformly bound (D; green). Control APTMS-tethered surfaces did not exhibit non-specific binding (E) and untreated glass slides were imaged under FITC conditions as a negative control for FITC-conjugated HA (F). Magnification: 20 × .

### 3.2.3. Elemental and chemical structure analysis of coated surfaces

The results of elemental and chemical structure analysis of treated substrates, as determined by XPS, are shown in Table 1, Table 2 and Fig. 5. XPS spectra generated on glass surfaces exhibited strong peaks for elemental silicon and oxygen, with carbon, calcium and sodium as minor contaminants. Tethering aminosilanes onto the surface reduced detection of silicon and oxygen while the elemental content of carbon and nitrogen was enhanced. The XPS elemental scan and high-resolution spectra generated by the

HA-coated surfaces varied as a function of their molecular weight, as will be discussed later. The high-resolution spectra for HA 1000 and HA 200 were quantitatively similar, as were those for HA 20 and HA 4mer. Therefore, only one spectra from each group was included.

### 3.3. Quantification of HA loss from the surface

#### 3.3.1. Toluidine blue assay

The amount of HA bound to the aminated glass surfaces was estimated from the decrease in absorbance due to loss

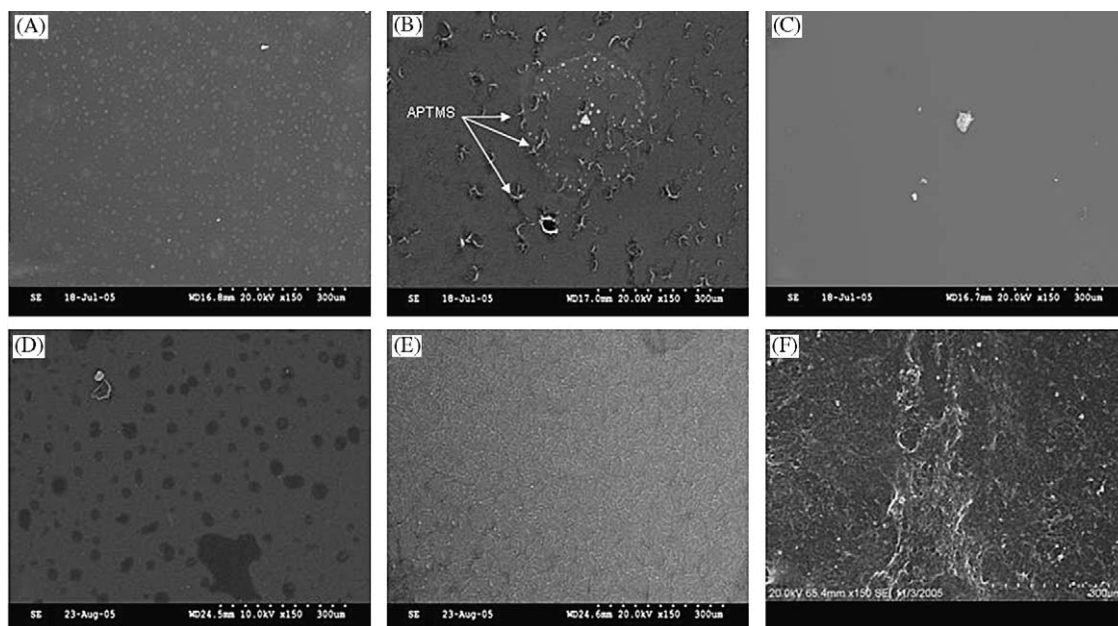


Fig. 3. Scanning electron micrographs of glass, APTMS, and HA-tethered surfaces. Glass surfaces appear smooth with spotted disfigurements attributed to the commercial plasma coating (A). Aminosilane-treated glass shows the presence of APTMS molecules (B). HA 200, HA 20 and HA 4mer appear as fibrous sheet-like networks (D–F) with some gaps within, while HA 1000 coated the surfaces as a smooth sheet without any detected morphology (C). Magnification:  $150\times$ .

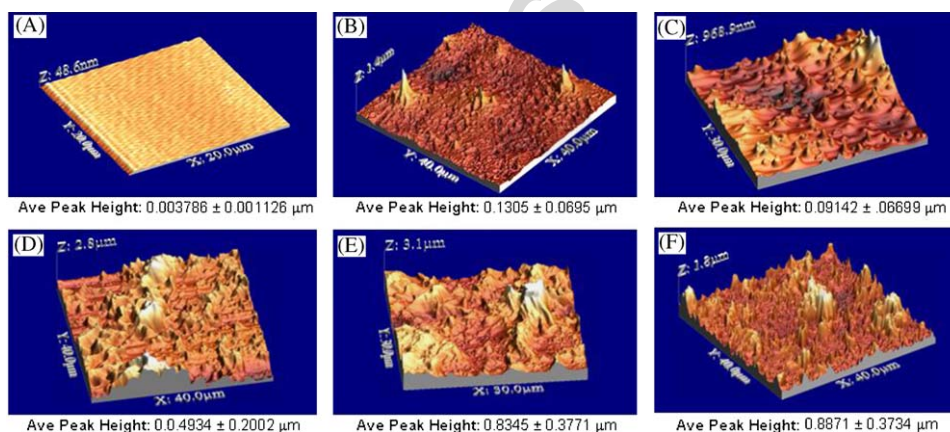


Fig. 4. Atomic force micrographs and the corresponding peak heights of glass, APTMS and HA-tethered surfaces. Glass surfaces appear very smooth with a consistent atomic topography (A). The addition of aminosilane to the glass surface resulted in a much rougher surface (B). The peak heights indicate that the HA surface roughness are inversely proportional to MW of tethered HA chains. In accordance, HA 1000 (C) and HA 200 (D) appear more smooth than HA 20 and HA 4mer.

Table 2  
High resolution C1s composition of the HA surfaces

Surface	XPS C1s composition (%)		
	CH	C–N/C–O	O–C–O/N–C=O
HA 1000	39.0	53.0	8.0
HA 200	13.7	76.4	9.9
HA 20	60.6	28.4	11.0
HA 4mer	57.3	27.6	15.1

A greater amount of C–N and lower quantity of N–C=O was detected on surfaces with larger HA fragments (HA 1000, HA 200) indicating a higher binding efficiency of the smaller HA fragments (HA 20, HA 4mer) with the silane-amines.

of toluidine blue from a contacting solution, by reaction with HA on the surfaces (Fig. 6). Absorbances of toluidine blue solution contacted with HA/fragment-tethered surfaces were consistently much lower than glass and amine-tethered surfaces, indicating successful immobilization of HA. A high absorbance was generated on glass ( $3.07 \pm 0.03$ ) and APTMS-treated surfaces ( $2.89 \pm 0.05$ ), similar to fresh toluidine blue solution ( $3.07 \pm 0.19$ ). Toluidine blue incubated with the HA 1000 surface exhibited absorbances ( $0.85 \pm 0.20$ ) much lower than that for both HA 200- and HA 20-tethered surfaces ( $1.60 \pm 0.38$ ,  $1.76 \pm 0.39$ ) and remained unchanged over 21 days of incubation of the substrate with culture medium. Retention

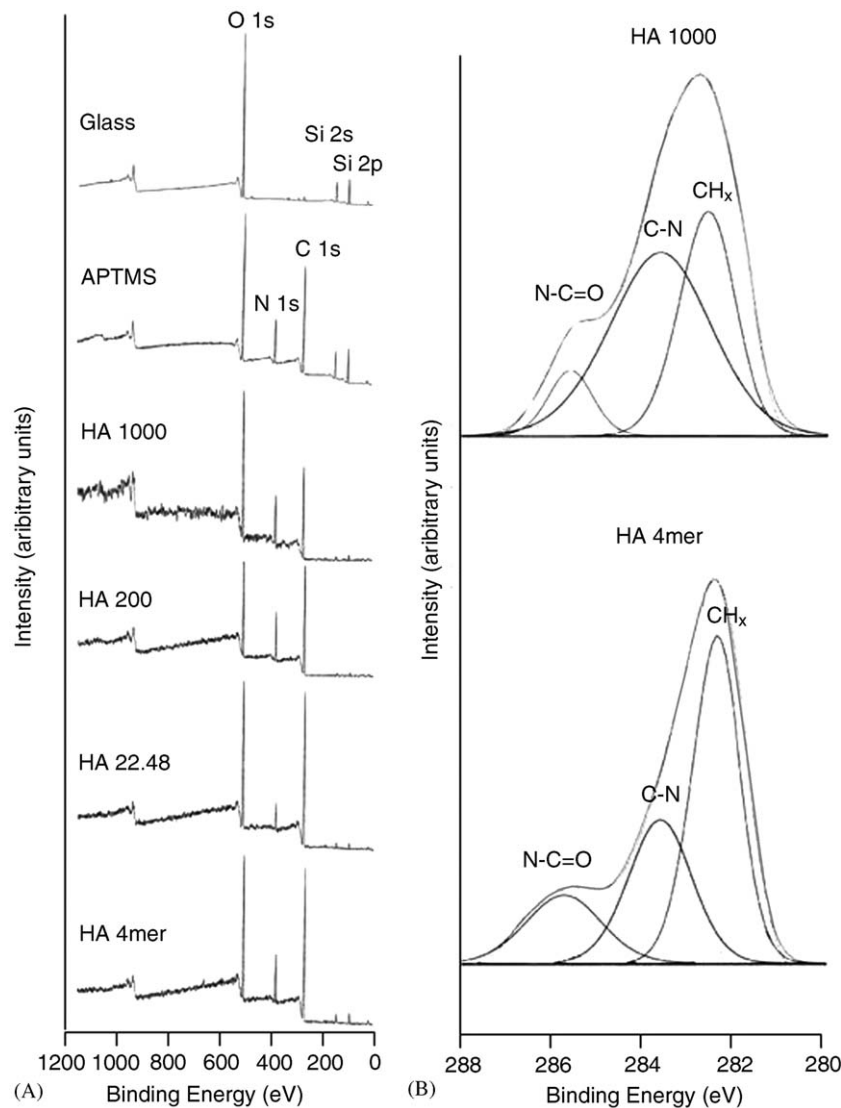


Fig. 5. XPS elemental scan and C1s high-resolution spectra of glass, APTMS and HA/fragments/oligomer-tethered surfaces. The prominent peaks observed corresponded to oxygen, silicon, nitrogen, and carbon (A). High-resolution spectra of the HA C1s peaks indicated that the relative amount of N-C=O functional groups was inversely proportional to MW of tethered HA chains (B). Presumably, this is due to the inefficient use of available surface amine groups by HMW HA for binding due to steric interference by entangling large HA chains.

of HA 4mer on surfaces was tested with toluidine blue only on 0 and 21 days of incubation with medium, and generated the highest absorbances of the HA surfaces ( $2.45 \pm 0.12$ ).

### 3.3.2. FACE analysis

FACE analysis was used to quantify the amount of HA present on surfaces (2 sq cm). At day 0, HA 1000-tethered surfaces contained approximately 9 times the amount of HA disaccharide units ( $9.36 \pm 1.68 \mu\text{g}$ ) than the other fragment sizes (Fig. 7). At day 0, HA 200, HA 20 and HA 4mer surfaces contained approximately the same amount of HA disaccharides ( $1.00 \pm 0.48$ ,  $1.31 \pm 1.15$ ,  $0.92 \pm 0.56 \mu\text{g}$ , respectively). These coated amounts remained unchanged after 21 days of incubation with

medium suggesting negligible loss from the surface irrespective of tested HA fragment size.

### 3.4. Cell proliferation

HA 1000, HA 200, HA 20 and HA 4mer-tethered surfaces did not incite significant proliferation of rat aortic ECs over 21 days of culture; the proliferation ratios were comparable to that obtained on the APTMS surfaces (negative controls; Fig. 8). None of the tested HA fragment sizes provided the necessary stimulus for vascular EC proliferation; proliferation ratios were much lower than that for positive control cultures, i.e., cells cultured on glass and fibronectin-coated glass.

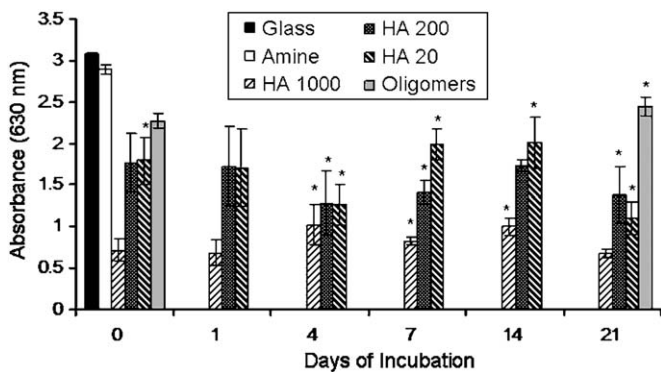


Fig. 6. Toluidine blue assay of glass, APTMS and HA-tethered surfaces. Irrespective of fragment size, tethered HA appears to be stably retained over 21 days of incubation with serum-free medium as evidenced by a lack of absorbance change (i.e., increase) of the toluidine blue solution. Higher molecular weights of HA were able to bind more toluidine blue molecules from the solution due to a greater number of availability of unreacted carboxyl groups. Values shown represent mean  $\pm$ SD of  $n = 4$  samples/substrate/incubation time.

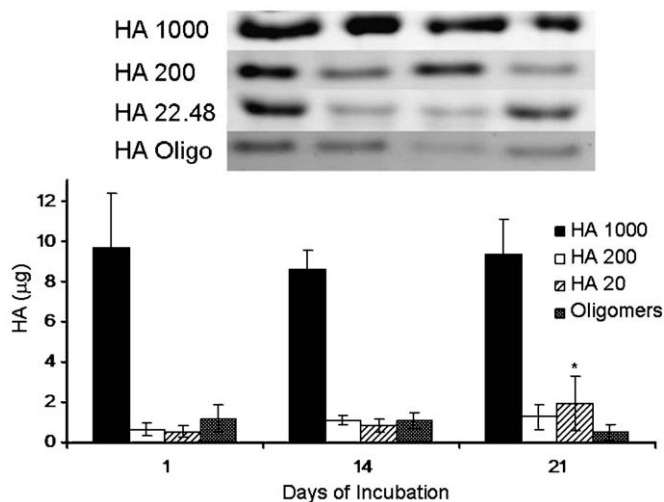


Fig. 7. FACE analysis of HA surfaces. More HA 1000 was present on the surface than the other molecular weights. The amount of HA 200, HA 20 and HA 4mer was similar. In all cases, the amount of HA was stable on the surfaces throughout the 21 days. Values shown represent the mean disaccharide content  $\pm$ SD of  $n = 4$  samples/substrate.

#### 4. Discussion

The long-term goal of our research is to develop HA-based scaffolds for vascular regeneration that will be conducive to the development of a normally functional luminal endothelium. A healthy and confluent EC lining is crucial to reinstate anti-thrombotic and anti-hyperplastic endothelial signaling pathways that are disrupted by vascular injury or disease.

The choice of HA as a vascular implant material stems from its biocompatibility and non-immunogenicity, an outcome of the high degree of homology in its structure across species [2], and its potential, as a ECM component, to evoke native, non-exaggerated responses from cultured vascular cells. HA has also been shown to exhibit

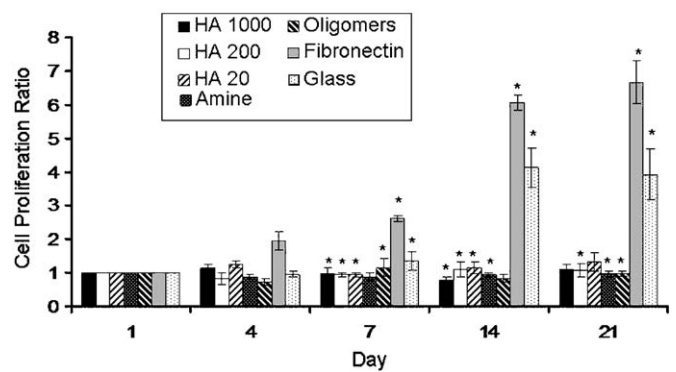


Fig. 8. Proliferation of rat aortic smooth muscle cells on glass, APTMS, HA/fragment/oligomers, and fibronectin surfaces. All HA surfaces inhibited cell proliferation when compared to glass and fibronectin and induced similar proliferation ratios as the APTMS substrate. Values shown represent the mean proliferation ratios  $\pm$ SD of  $n = 4$  samples/substrate.

angiogenic tendencies, although these effects, as with other phenomena observed with other cell types, appear to be highly specific to HA fragment size [3]. In our previous work, we have also seen that cells respond to HA oligomers more exuberantly than to larger sized HA, and show significant size-specificity in their responses, even within the oligomer size range. However, other studies have also shown HA fragments and HA oligomers to be capable of inducing inflammatory responses [2]. Thus, the distribution of bioactive HA fragments and oligomers within a HA-based scaffold must be defined and optimized to elicit desired outcomes (i.e., functional endothelialization) and prevent unwanted ones (i.e., inflammation). We thus seek to comprehensively determine the specific fragment-size effects of HA on ECs.

In a prior study [10], we determined that a model of exogenous HA/fragment supplementation inadequately predicted cell responses to a HA-based scaffold, likely due to the absence of cell-HA/fragment contact. Since fragmented HA/oligomers cannot by themselves be cross-linked into solid hydrogels to test their stand-alone impact on EC responses, we have developed a surface-tethered model of HA to test HA fragment-size specific EC responses.

Silane coupling agents are often used to durably link organic, and inorganic groups such as those present on glass. We chose to use a aminotrialkoxysilane due to its presentation of an exposed  $-\text{NH}_2$  group and its hydrolytic stability [14]. Trialkoxysilanes form 3D silane networks of bonded multilayers on the glass surface that restrict the infiltration of hydrolytic substances from solution. If necessary, however, silanes incorporating even more hydrolysis-resistant aromatic groups may be used in the future.

Among the chemically reactive groups on HA ( $-\text{OH}$ ,  $-\text{COOH}$ ) [15], we targeted the carboxyl groups specifically due to their ability to react with primary amines. To do this, the carboxyl groups of the component HA

disaccharide monomers were activated with EDC into the chemically reactive and unstable *O*-acylisourea. This complex can either react with a primary amine to form stable amide bonds or undergo hydrolysis in the presence of water to reform the carboxyl. To prevent the hydrolysis of *O*-acylisourea, NHS is added to the solution. NHS combines with *O*-acylisourea to form a semi-stable and amine reactive NHS-ester to increase the efficiency of EDC-mediated coupling reactions [16]. In the past, some studies have used charged sulfo-NHS instead of NHS because of its increased solubility. No experiments were conducted to compare the solubility and relative reactivity of these molecules but NHS was found to readily and completely solubilize in aqueous solutions and, therefore, was used in these experiments. Although no concrete proof is available, one previous study expressed doubts in a similar method of HA immobilization based on XPS results that deviated from the expected theoretical values. Therefore, we have presently characterized the created aminosilane and HA-tethered surfaces using various analytical techniques.

Analysis of the HA surfaces by fluorescence, SEM and AFM indicate that at the level of cell size (~10–20  $\mu\text{m}$ ), the HA coatings are highly homogeneous and continuous. Results of XPS analysis correctly reflected the changes in surface-elemental composition that might be expected to occur upon aminosilane treatment and HA immobilization. However, the relative content of these elements showed slight differences from that might be theoretically expected based on the stoichiometry of HA, likely due to steric hindrance. Upon aminosilane treatment, an expected increase in nitrogen and carbon content was observed. The elemental profiles were similar to that theoretically expected APTMS. Assuming complete reaction of all tethered amine groups on the surface to the carboxyl groups on HA, the % elemental composition of HA-tethered substrates should be independent of their molecular weight. Yet, the XPS results show differences in elemental composition between HA 1000, HA 200, HA 20 and HA 4mer surfaces. Specifically, as seen in Table 1, the % composition of nitrogen atoms on HA 1000- and HA 200-tethered surfaces was somewhat higher than that of HA 20 and HA 4mers (11.2%, 10.7% vs. 5.0%, 8.3%). We believe that these differences stem from the greater gaps within the higher MW HA coatings and the less efficient binding to available tethered amine groups. High-resolution XPS analysis confirms this since a higher % content of C–N and lower N–C=O bonding functionalities were detected for HA 1000 and HA 200 relative to the other sized HA fragments.

When a single disaccharide unit of polymeric HMW HA binds to an APTMS amine, the remaining strand may effectively prevent other such strands from binding to the APTMS molecules in the local vicinity by directly binding to them or sterically inhibiting their interaction with other strands. As a result, binding of HMW HA to surface amines is less efficient. It is also possible that the large size

of the HMW HA strands also causes substantial strand entanglement to produce a compact zone of HA close to the aminated surface, yet creating sporadic gaps devoid of HA. This theory was supported by our low magnification immunofluorescence micrographs which indicated areas of intense fluorescence, likely due to large HA strands stacked on top of one another, adjoining darker ones (gaps/pores) less densely covered with HA. Such a distribution of HA could more easily permit the detection of un-reacted, exposed nitrogen containing amine groups, to thus increase the elemental concentration of nitrogen above that expected theoretically. With regard to shorter HA fragments, such entanglement and steric hindrance were apparently far less of an issue as evidenced by fluorescence detection of uniform intensity, and much lower levels of detection of APTMS amines and a higher degree of C–N=O structures by XPS, which suggest more efficient reaction between APTMS amines and HA. Also, when imaged under high magnification (SEM), a fibrous surface was revealed, with clustered short HA fibers. Likely, these fibers were concentrated around the APTMS amine functional groups preventing their detection. In support of these observations, AFM data indicate higher peaks on surfaces tethered with HA 20 and HA 4mer than that tethered with HA1000 and HA 200. This suggests the shorter HA fragments were not entangled with one another to create a compact zone, but rather individually attached to the amines.

The FACE outcomes support our hypothesis that HA 1000 forms entangled networks on the surface, unlike shorter HA fragments and oligomers; indeed, the amount of HA 1000 immobilized on glass was far greater than that of HA 200, 20 or HA 4mer. Shorter HA fragments likely do not stably entangle with one another due to their smaller size. Thus excess fragments were released from the surface when rinsed immediately after preparation but just prior to incubation with medium.

FACE and the toluidine blue assay both confirmed the long-term (21 days) retention of the immobilized HA/fragments/oligomers but each used a different process. FACE directly measures the amount of enzyme-digested tethered HA, while the toluidine blue assay utilizes an indirect approach. Toluidine blue binds to carboxyl groups present on HA disaccharides [17]. Since the number of disaccharides in each case is dependant on HA chain length, tethered amount between different HA size groups. However, for each HA size we can reliably monitor the retention of HA/fragments/oligomers on the surface over time.

Since cells cultured on an HA scaffold would encounter HA as a substratum and not freely diffusing HA molecules, we sought to create HA-substrates that would somewhat replicate this environment. Yet, the results indicate that HA, bound utilizing the available carboxyl functional groups, does not promote EC proliferation. This could have multiple possible causes. Firstly, the carboxyl groups, used to immobilize the HA, may be crucial for the

stimulation of EC receptors. Small HA fragments have a limited number of carboxyl groups and most of them are utilized in the immobilization procedure, preventing their interaction with cells and thus, inhibiting EC anchorage and proliferation. Larger HA fragments contain more carboxyl groups available for cell interaction but suffer from high charge densities and smooth surface topographies; both of which are known to inhibit cell adhesion [18,19].

Although the reasons for the unique interactions of different sized HA fragments with ECs is unclear, it is believed to be due to their differential interactions with cell surface receptors specific for HA. CD44 is a transmembrane adhesion receptor found in several cell types, including ECs, and is the most studied among three cell membrane receptors for HA currently identified, the others being Receptor for HA Mediated Motility (RHAMM), and Toll-Like Receptor 4 (TLR4) [20]. Studies have shown that HA oligomers can incite very different cell responses when bound to CD44 receptors, than when HMW HA interacts with them, because HA oligomers can cause clustering of multiple CD44 receptors and thus alter intracellular responses [21]. The stimulation of CD44 receptors by HA oligomers has also been suggested to enhance the production of vascular EC growth factor (VEGF) and therefore promote EC proliferation [22]. The CD44 receptor is also known to mediate cellular adhesion [23]. Studies have shown that the smallest HA oligomer capable of interacting with CD44 is 6mer [24]; 4mer have their own receptor, identified as TRL4. Since HA oligomers of slightly different sizes can potentially elicit conflicting cell responses, and in light of the difficulty and high cost of procuring pure, single-sized HA oligomers, in the current feasibility study, we created a rough HA digest composed predominantly (75% w/w) of oligomers of single size (4mers), that uniquely interact with receptors (TRL4) which are not influenced by larger oligomers in the digest. Also, in a parallel study in our laboratory, identically generated and immobilized HA 4mer were shown to encourage adherence and elastin production of smooth muscle cells (unpublished lab results). While the exact function of the 4mer receptor is unknown, it appears that its interaction with the HA 4mer does not stimulate endothelial proliferation in the manner elicited by interactions of larger oligomers (6–12mers) with CD44. Future studies will therefore investigate the effects of these larger HA oligomers using the currently described culture model.

## 5. Conclusion

One of the main obstacles in vascular graft development is the regeneration of a confluent EC layer on the luminal surface. These results indicate that immobilized HA oligomers, utilizing the carboxyl functional group, do not provide the necessary stimulus for EC regeneration. This is, in part, due to the high 4-mer content in our prepared oligomer mixtures that interacted with a non-CD44

receptor that apparently has no effect on EC proliferation, although stimulatory effects have been seen with other cells. Yet, this immobilization technique is useful towards determining the size- and dose-specific responses of surface-tethered HA on EC responses and tailoring the design of HA scaffolds suited to vascular tissue engineering applications. These studies will form the basis for future work in our lab, aimed towards development of HA-based vascular graft materials.

## Acknowledgements

The authors thank Dr JoAn Hudson, director of the Clemson Electron Microscope Facility, Anderson, SC, for her assistance with the SEM and XPS work presented in this study. This work was supported by funding from the National Institutes of Health (P20RR-016461, C06RR01882), the National Science Foundation (0132573) and the American Heart Association (SDG 0335085N).

## References

- [1] Tan SW, Johns MR, Greenfield PF. Hyaluronic acid—a versatile biopolymer. *Aust J Biotechnol* 1990;4:38–43.
- [2] Chen WY, Abatangelo G. Functions of hyaluronan in wound repair. *Wound Repair Regen* 1999;7:79–89.
- [3] Morra M. Engineering of biomaterials surfaces by hyaluronan. *Biomacromolecules* 2005;6:1205–23.
- [4] Pavesio A, Abatangelo G, Borrione A, Brocchetta D, Hollander AP, Kon E, et al. Hyaluronan-based scaffolds (Hyalograft C) in the treatment of knee cartilage defects: preliminary clinical findings. *Novartis Found Symp* 2003;249:203–17 (discussion 29–33, 34–8, 39–41).
- [5] Price RD, Myers S, Leigh IM, Navsaria HA. The role of hyaluronic acid in wound healing: assessment of clinical evidence. *Am J Clin Dermatol* 2005;6:393–402.
- [6] West DC, Chen H. Is hyaluronan degradation an angiogenic/metastatic switch? In: Kennedy JF, Phillips GO, Williams PA, Hascall V, editors. *Hyaluronan*. Cambridge, UK: Woodhead Publishing Ltd; 2002. p. 165–72.
- [7] West DC, Kumar S. The effect of hyaluronate and its oligosaccharides on endothelial cell proliferation and monolayer integrity. *Exp Cell Res* 1989;183:179–96.
- [8] Feinberg RN, Beebe DC. Hyaluronate in vasculogenesis. *Science* 1983;220:1177–9.
- [9] Ramamurthi A, Vesely I. Ultraviolet light-induced modification of crosslinked hyaluronan gels. *J Biomed Mater Res A* 2003;66:317–29.
- [10] Joddar B, Ramamurthi A. Elastogenic effects of exogenous hyaluronan oligosaccharides on vascular smooth muscle cells. *Biomaterials* 2006;27:5698–707.
- [11] Stile RA, Barber TA, Castner DG, Healy KE. Sequential robust design methodology and X-ray photoelectron spectroscopy to analyze the grafting of hyaluronic acid to glass substrates. *J Biomed Mater Res* 2002;61:391–8.
- [12] Calabro A, Benavides M, Tammi M, Hascall VC, Midura RJ. Microanalysis of enzyme digests of hyaluronan and chondroitin/dermatan sulfate by fluorophore-assisted carbohydrate electrophoresis (FACE). *Glycobiology* 2000;10:273–81.
- [13] Labarca C, Paigen K. A simple, rapid, and sensitive DNA assay procedure. *Anal Biochem* 1980;102:344–52.
- [14] Matinlinna JP, Lassila LV, Ozcan M, Yli-Urpo A, Vallittu PK. An introduction to silanes and their clinical applications in dentistry. *Int J Prosthodont* 2004;17:155–64.

- [15] Balazs EA, Bland PA, Denlinger JL, Goldman AI, Larsen NE, Leshchiner EA, et al. Matrix engineering. *Blood Coagul Fibrinolysis* 1991;2:173–8.
- [16] Staros JV, Wright RW, Swingle DM. Enhancement by *N*-hydroxysulfosuccinimide of water-soluble carbodiimide-mediated coupling reactions. *Anal Biochem* 1986;156:220–2.
- [17] Johnston JB. A simple, nondestructive assay for bound hyaluronan. *J Biomed Mater Res* 2000;53:188–91.
- [18] Chung TW, Liu DZ, Wang SY, Wang SS. Enhancement of the growth of human endothelial cells by surface roughness at nanometer scale. *Biomaterials* 2003;24:4655–61.
- [19] Lee JH, Lee JW, Khang G, Lee HB. Interaction of cells on chargeable functional group gradient surfaces. *Biomaterials* 1997;18:351–8.
- [20] Aruffo A, Stamenkovic I, Melnick M, Underhill CB, Seed B. CD44 is the principal cell surface receptor for hyaluronate. *Cell* 1990;61:1303–13.
- [21] Liu D, Liu T, Li R, Sy MS. Mechanisms regulating the binding activity of CD44 to hyaluronic acid. *Front Biosci* 1998;3:d631–6.
- [22] Murphy JF, Lennon F, Steele C, Kelleher D, Fitzgerald D, Long AC. Engagement of CD44 modulates cyclooxygenase induction, VEGF generation, and proliferation in human vascular endothelial cells. *Faseb J* 2005;19:446–8.
- [23] Savani RC, Cao G, Pooler PM, Zaman A, Zhou Z, DeLisser HM. Differential involvement of the hyaluronan (HA) receptors CD44 and receptor for HA-mediated motility in endothelial cell function and angiogenesis. *J Biol Chem* 2001;276:36770–8.
- [24] Evanko SP, Angello JC, Wight TN. Formation of hyaluronan- and versican-rich pericellular matrix is required for proliferation and migration of vascular smooth muscle cells. *Arterioscler Thromb Vasc Biol* 1999;19:1004–13.

Author's personal copy